CHAPTER 3

THEORETICAL ANALYSIS OF HETEROJUNCTIONS

As previously described in Chapter 2, a heterojunction, in general is defined as the interface between two dissimilar materials. If the two semiconductors involved have similar types of conductivity, then the junction is called isotype heterojunction, otherwise it is called anisotype heterojunction. This chapter outlines the theoretical background, specifically to the Mo/Cu(In,Ga)Se_2/CdS/ZnO heterojunction thin film solar cells.

3.1 Heterojunction Solar Cell

The use of a heterojunction with a large band-gap window material and a small band-gap absorber material is used to minimize the surface recombination. The use of heterojunction expands the semiconductor material possibilities for solar photovoltaics. The carrier transport properties of heterojunctions are generally dominated by phenomena in the interface region. The current transport in the depletion layer is variously attributed to recombination, tunneling, or combination of tunneling and recombination involving energy levels near the interface.

3.1.1 Energy band profiles for p-n heterojunction [4]

The typical band diagrams for p-n heterojunction are given in Figs. 3.1-3.3, where the p-type material is assumed to have a smaller band gap than that of the

n-type material. A variety of complex phenomena can occur at the junction interface, following the Anderson abrupt-junction model.

The two semiconductors are assumed to have different energy gaps E_g, different dielectric constant ε, different work function ϕ, and different electron affinities χ. The electron affinity and work function of a given semiconductor are defined, respectively, as that energy required to remove an electron from the conduction band and from Fermi level to a position just outside the material.

Various possible equilibrium energy band profiles and related information for p-n heterojunctions having $E_{g1} < E_{g2}$:

Case I **anisotype junction with no conduction or valence band spike** [4]

Conditions: $\chi_1 < \chi_2 < \chi_1 + E_g$,

$\phi_1 > \phi_2$.

Current-voltage relation: $$I = B\exp\left[-\frac{q(\Delta E_C + V_D)}{kT}\right]\times\left[\exp\left(\frac{qV}{kT}\right)-1\right], \qquad (3.1)$$

the total built-in voltage V_D, is equal to the sum of the partial built-in voltage:

$$V_D = V_{D1} + V_{D2} ,$$

where V_{D1} and V_{D2} are the electrostatic potential supported at equilibrium by semiconductor 1 and 2, respectively

and

$$\Delta E_C = \chi_2 - \chi_1 ,$$

$$B = aqXN_{D2}\left(\frac{D_{n1}}{\tau_{n1}}\right)^{1/2} ,$$

where X is the transmission coefficient for electrons across the interface, a is the junction area, D_{n1} and τ_{n1} are diffusion constant and life-time, respectively.

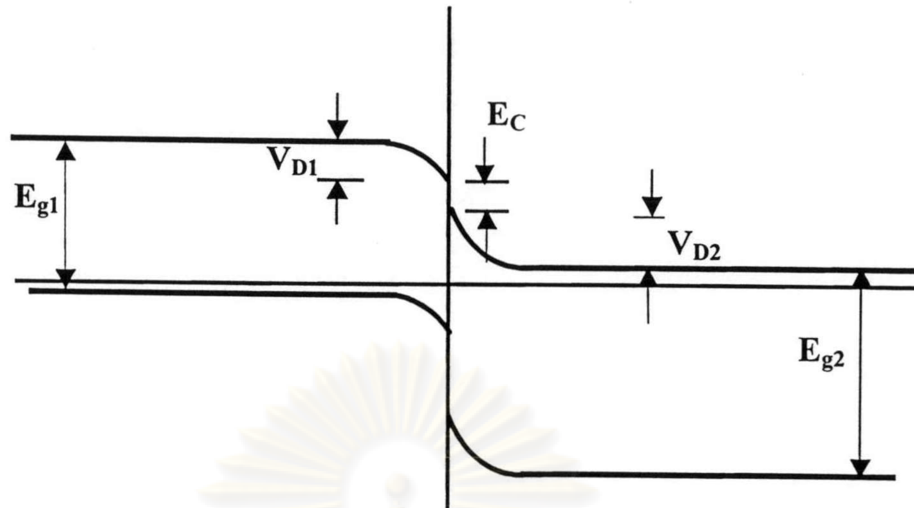

Figure 3.1: Equilibrium energy band profile case I .

Case I presents the usual configuration for a solar cell, with the desirable assumption that $\chi_1 < \chi_2$, thus the energy spike does not occur in the conduction band impeding electron transport from the p- to the n-type.

Case II **anisotype junction with conduction band spike** $(V_{D1} > \Delta E_C)$ [4]

For the p-n heterojunction, the predominant current will be electrons because the barrier for electrons is much smaller than that for holes.

Conditions: $\chi_1 > \chi_2$,

$\phi_1 > \phi_2$,

$\chi_1 + E_{g1} < \chi_2 + E_{g2}$,

Neglecting the generation-recombination current, the current-voltage relation is given by

$$I = B\exp\left[-\frac{q(V_D - \Delta E_C)}{kT}\right] \times \left[\exp\left(\frac{qV}{kT}\right) - 1\right] , \qquad (3.2)$$

where V_1 and V_2 are the portions of the applied voltage appearing in p- and n-type semiconductors, $\Delta E_C = \chi_1 - \chi_2$,V_D, V, and B are the same as in case I. Under forward bias, $V_{D1} - V_1 < \Delta E_C$:

$$I = B\exp\left[-\frac{q(V_{D2})}{kT}\right]\times\left[\exp\left(\frac{qV_2}{kT}\right)-\exp\left(-\frac{qV_1}{kT}\right)\right]. \tag{3.3}$$

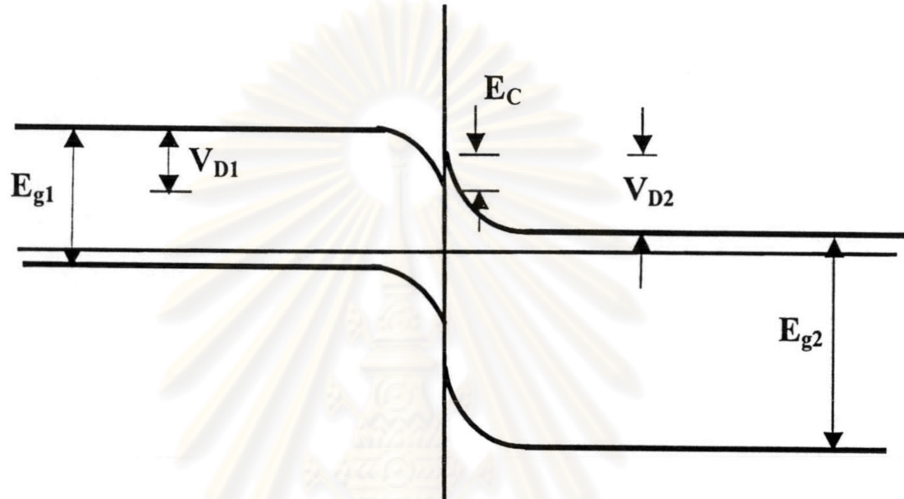

Figure 3.2: Equilibrium energy band profile case II .

<u>**Case III**</u> **anisotype junction with conduction band spike** $(V_{D1} < \Delta E_C)$ [4]

Conditions: $\chi_1 > \chi_2$,

$\phi_1 > \phi_2$,

$\chi_1 + E_{g1} < \chi_2 + E_{g2}$.

Neglecting the generation-recombination current, the current-voltage relation is given by

$$I = B\exp\left[-\frac{q(V_{D2})}{kT}\right]\left[\exp\left(\frac{qV_2}{kT}\right)-\exp\left(-\frac{qV_1}{kT}\right)\right], \tag{3.4}$$

ศูนย์วิทยทรัพยากร
จุฬาลงกรณ์มหาวิทยาลัย

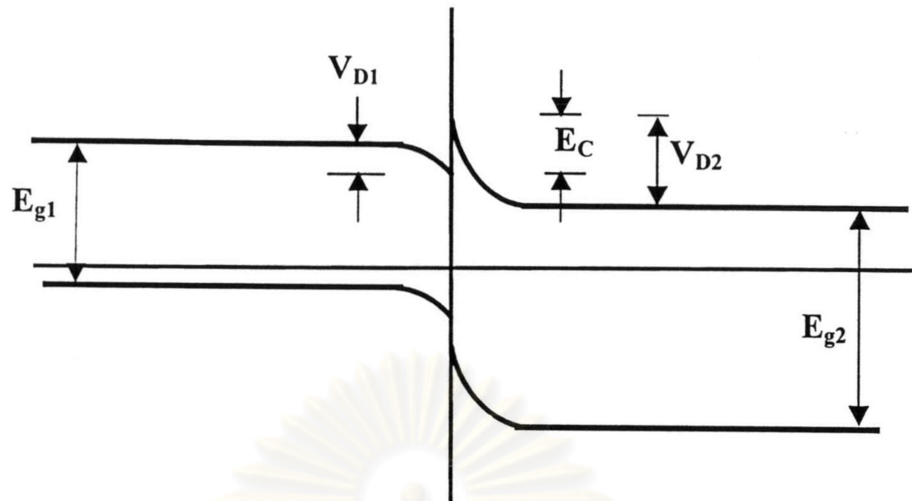

Figure 3.3: Equilibrium energy band profile case III .

where V_1 and V_2 are the portions of the applied voltage appearing in p- and n-type semiconductors, $\Delta E_C = \chi_1 - \chi_2$ and V_D, V, B are the same as in case I. Under reverse bias, $V_{D1} + |V_1| > \Delta E_C$:

$$I = B\exp\left[-\frac{q(V_D - \Delta E_C)}{kT}\right] \times \left[\exp\left(\frac{q|V|}{kT}\right) - 1\right]. \tag{3.5}$$

In case III, hole transport across the interface to recombination in the n-quasi neutral region is negligible with respect to the electron current because of the large barrier for holes.

3.1.2 The Effect of Interface States on Electrical Properties of Heterojunction

The presence of a large density of interface states provides two mechanisms in heterojunctions:

1. The charge stored in the states distorts the band profile, raising or lowering the conduction bands at the interface with respect to the equilibrium Fermi level, the magnitude of the charge can be measured by capacitance-voltage (C-V) techniques.

2. The states provide a large density of recombination centers result in the high dark diode current values observed.

In many cases, the extremely high density of charged states at specific energy levels at the surface is sufficient to pin the surface (or interface) Fermi level at that energy. In general, the states responsible for pinning the Fermi level at a free surface are different, depending on the majority carrier type (acceptor-like for n-type and donor-like for p-type materials)

3.1.3 Transport mechanism in heterojunction solar cell

Analysis of thin film polycrystalline heterojunction solar cells involves the current loss mechanism of devices and the energy band profile.

It is assumed that the illuminated current-voltage characteristics can be written as[7]

$$J = J_L - J_D \tag{3.9}$$

$$J_D = J_0 \exp\left(\frac{q(V - R_s J)}{AkT}\right) + \frac{(V - R_s J)}{R_{sh}} \tag{3.10}$$

where J_L is the light generated current, J_D is diode current accounts for normal current loss, R_s is the series resistance, R_{sh} is the shunt resistance, J_0 is the reverse saturation current, and A is the diode ideality factor. The magnitude of the two current-loss terms depends on the voltage across the junction V_j;

$$V_j = V - R_s J, \tag{3.11}$$

where V is the voltage across the load and J is the current through the load. The interpretation of experimental data has been accomplished with one diode like term

and a shunt resistance term. To achieve a high efficiency solar cell, the diode current J_D must be made as small as possible.

The J-V parameters, J_0 and A vary with temperature or have characteristic values which suggest the dominant current loss mechanism. In all p-n junction, several current transport mechanisms (transport of holes and electrons across the depletion region) can be presented at the same time. Such transport mechanisms in the forward bias direction include injection of carriers over the junction barrier, recombination of holes and electrons within the depletion region, and injection of carriers up a portion of the barrier followed by tunneling into energy states within the band gap.

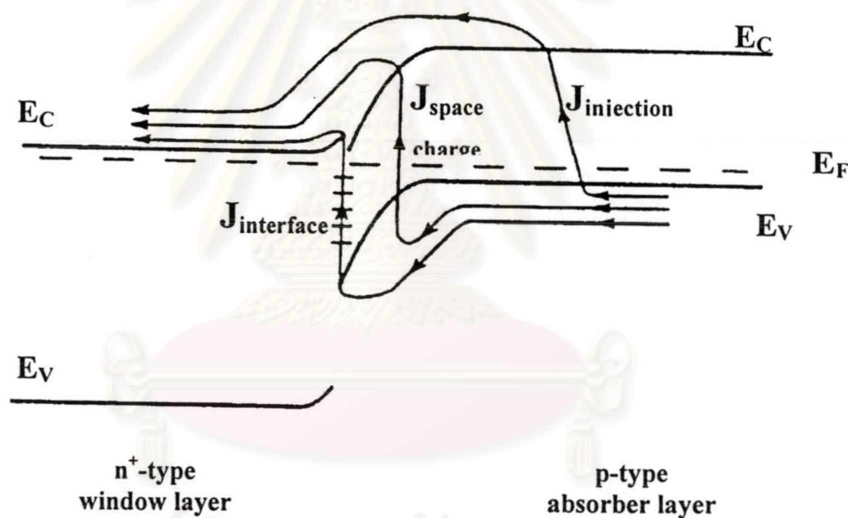

Figure 3.4: Energy band schematic of the diode current in a heterojunction cell. Three current transport mechanisms in forward bias: (1) the injection current; (2) the recombination current within the space charge region; and (3) the recombination current at the metallurgical interface [8].

Figure 3.4 shows the possible current transport mechanism in forward bias. The following describe the three current transport mechanism:

1. Injection currents

The injected current component consists of electrons injected from the n-side over the potential barrier into the p-side, where they diffuse and drift away from the junction. The current component also consists of an analogous current due to holes injected from the p-side into the n-side. After injection and diffusion, recombination finally occurs away from the junction. The injection current can be expressed as [9]

$$J_{inj} = J_0\left[\exp\left(\frac{qV}{kT}\right)-1\right], \tag{3.12}$$

$$J_0 = q\left(\frac{n_i^2}{N_A}\right)\left(\frac{L_n}{\tau_n}\right), \tag{3.13}$$

where, in the p-type material, n_i is the intrinsic carrier density, N_A is the acceptor density, L_n is the electron diffusion length, and τ_n is the electron lifetime.

2. Space charge region recombination current

When a p-n junction is forward biased, electrons from the n-side and holes from the p-side are injected across the junction depletion region into p-and n-sides, respectively. At the same time some of these carriers recombine inside the depletion region resulting in an increase in the dark current through the device. The recombination rate expression is used based on Shockley-Read-Hall (SRH) recombination via a single trap within the band gap (as previously described in chapter 2). The space charge region recombination current can be expressed as [9]

$$J_{rec} = J_0\left[\exp\left(\frac{qV}{AkT}\right)-1\right], \tag{3.14}$$

$$J_0 = \frac{qn_i}{\left(\tau_{n0}\,\tau_{p0}\right)^{1/2}}\frac{\pi kTw}{4(\phi - V)}, \tag{3.15}$$

where w is the width of space charge region, ϕ is the potential barrier, τ_{n0} is the electron lifetime and τ_{p0} is the hole lifetime. The value of diode ideality factor A is approximately 2 and independent of temperature. For an exponential defect distribution, A is temperature dependent and lies between 1 and 2.

3. Interface recombination current

The interface of metallurgical is expected to be characterized by a high density of band gap states. The recombination occurs through interface states. The interface recombination current can be expressed as [9]

$$J_{\text{int}} = J_0\left[\exp\left(\frac{qV}{kT}\right)-1\right]. \tag{3.16}$$

For an asymmetrically doped junction ($N_D > N_A$), the diode ideality factor A is constant and can be expressed as [10]

$$A = 1+\frac{N_A}{N_D}, \tag{3.17}$$

where N_A is the density of acceptor and N_D is the density of donor.

The third type of dark diode current component can exist under two situations to determine J_0:

- The current is limited by the diffusion of holes when the interface recombination velocity s_I is larger than the thermal velocity of electron v_{th}. In this case, J_0 can be expressed as the expression for thermionic emission;

$$J_0 = \left(\frac{4\pi q m_h^*}{h^3}\right)(kT)^2 \exp\left(-\frac{q\phi}{kT}\right). \tag{3.18}$$

- As the interface recombination velocity s_I is smaller than the thermal velocity v_{th}, J_0 can be expressed as [9]

$$J_0 = qs_I N_v \exp\left(-\frac{q\phi}{kT}\right) = (qS_I N_I v_{th})N_v \exp\left(-\frac{q\phi}{kT}\right), \tag{3.19}$$

where S_I is the electron capture cross section of interface states, N_I is the density of interface states.

The interface recombination current in Fig. 3.4 can exist under the interface recombination with tunneling situation. Since various traps may involve in the recombination at interface states, tunneling effects will dominate. Considering

although the band bending works as barrier for holes tunneling into interface states, the holes with energy enhanced by thermal excitation can tunnel through the barrier into electron-occupied interface states. The current is given by [9]

$$J_{tat} = J_0\left[\exp\left(\frac{qV}{AkT}\right)-1\right], \quad (3.20)$$

with

$$J_0 = J_{00}\exp\left[-\frac{qE_a}{AkT}\right], \quad (3.21)$$

$$A = \frac{E_{00}}{kT}\coth\left(\frac{E_{00}}{kT}\right), \quad (3.22)$$

$$E_{00} = \frac{qh}{4\pi}\left(\frac{N_A}{\varepsilon m_h^*}\right)^{1/2}, \quad (3.23)$$

where E_a is the activation energy, E_{00} is the characteristic tunneling energy, ε is the semiconductor's dielectric constant. The tunneling processes commonly dominate junction currents in the heterojunction at lower temperature.

As shown in Fig. 3.4, the main contributions to dark current or diode current J_D come from the injected electron current, the recombination current in the space charge region, and the recombination current at the metallurgical interface. By measuring J_D as a function of temperature and voltage the differences in A and ϕ enable to determine which of the current mechanisms is controlling J_D. The barrier height can usually be found by measuring V_{oc} as a function of temperature.

3.2 Cu(In,Ga)Se$_2$-Based Heterojunction Solar Cell

Among the more complex materials, the I-III-VI$_2$ compounds as well as their alloys, such as CuInSe$_2$/CdS and Cu(In,Ga)Se$_2$/CdS, are the most potential candidate for photovoltaic applications because of their demonstrated high solar

efficiencies 18.8% on the laboratory scale [11, 12]. $CuInSe_2$ has a direct band gap of 1.04 eV. Its chalcopyrite structure with lattice constant a = c/2 = 5.782 °A makes a good match to wurtzite CdS with a = 5.850 °A with only 1.2% lattice mismatch [9].

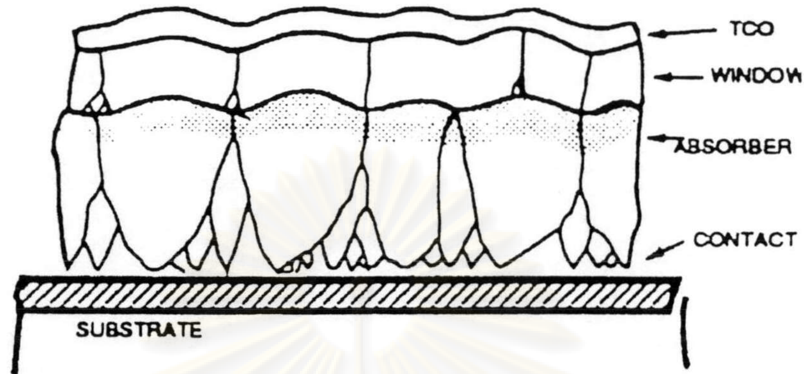

Figure 3.5: Cross section of a polycrystalline cell [8].

Schock et al.[13] proposed the transport model and the band diagram of $Cu(In,Ga)Se_2$-based thin film solar cell as shown in Fig. 3.6.

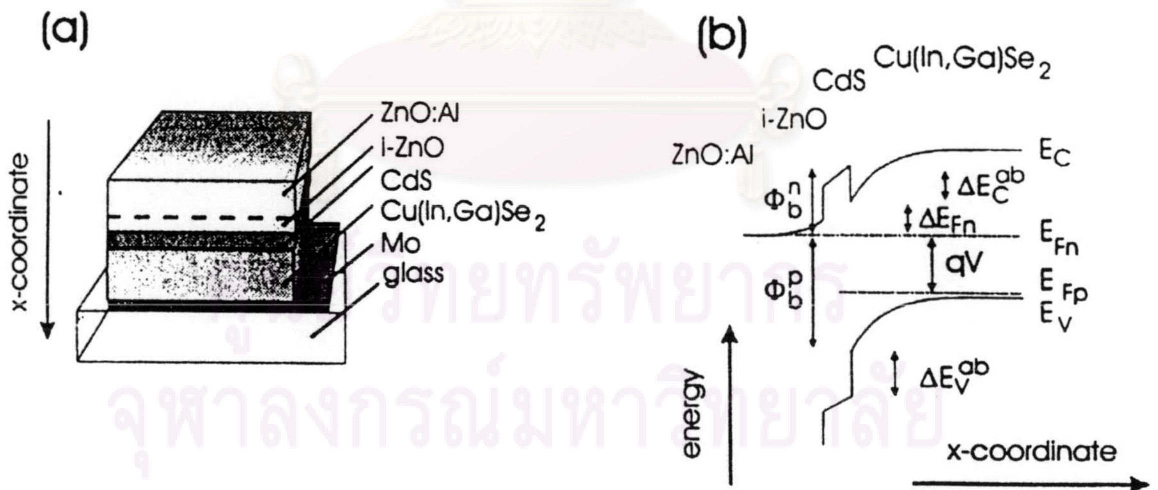

Figure 3.6: (a) The different layers of a $ZnO/CdS/Cu(In,Ga)Se_2$ heterojunction solar cell. (b) Band diagram of the heterojunction [13].

Figure 3.6 (b) shows the band diagram of the $ZnO/CdS/Cu(In,Ga)Se_2$ heterojunction with the conduction and valence band energies E_C and E_V, an

applied bias voltage V. ϕ_b^p, ϕ_b^n denote the barriers for holes and electrons. ΔE_{Fn} is the energy distance between the Fermi level and the conduction band energy at the CdS/Cu(In,Ga)Se_2 interface. ΔE_V^{ab} and ΔE_C^{ab} are the valence band and conduction band discontinuities at the buffer absorber interface.

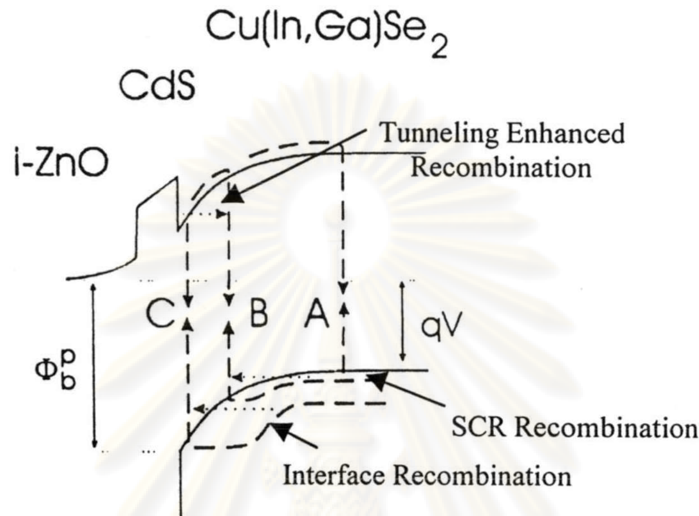

Figure 3.7: Band diagram under applied bias voltage showing the recombination paths. The dotted arrows indicate tunneling enhanced process, both at the interface and in the space charge region [14].

Figure 3.7 shows the recombination current processes in the ZnO/CdS/ Cu(In,Ga)Se_2 heterojunction which consists of the tunneling enhanced recombination in the space charge region and the tunneling enhanced interface recombination.

1. Tunneling enhanced interface recombination

At the buffer/absorber (n^+-p) interface where the electron concentration is larger than the free hole concentration, the large density of electron is available in the buffer layer. The resulting recombination current can be expressed as Eqs. (3.20) - (3.23).

I 2069166X

2. Tunneling enhanced bulk recombination

Assume an exponential distribution of recombination centers with maximum at the valence or conduction band edge. The recombination current depends on the density of defects in the bulk of the absorber material and on the built-in electrical field at the junction. The recombination current density via recombination centers in the space charge region is given by [14,15]

$$J = J_0 \exp\left(\frac{qV}{AkT}\right), \tag{3.24}$$

$$J_0 = J_{00} \exp\left(\frac{-E_g}{AkT}\right), \tag{3.25}$$

where V is applied voltage, A is the diode ideality factor, kT/q is the thermal voltage, E_g is the band gap energy of the absorber, and J_{00} is a prefactor depending on the transport mechanism (tunneling or thermal activation).

For recombination without tunneling, A can be written as [15]

$$\frac{1}{A} = \frac{1}{2}\left(1 + \frac{T}{T^*}\right). \tag{3.26}$$

The expression for A of Eq. (3.26) explains A which are between 1 and 2 for temperatures $0 < T < T^*$. However, at lower temperature the tunneling becomes more significant and the expression for A deviates from Eq. (3.26).

For recombination with tunneling, A can be expressed as [11,14,15]

$$\frac{1}{A} = \frac{1}{2}\left(1 - \frac{E_{00}^2}{3(kT)^2} + \frac{T}{T^*}\right), \tag{3.27}$$

where $E^* = kT^*$ is the characteristic energy of an exponential distribution of trap states and with the characteristic tunneling energy $E_{00} = \left(\frac{q\hbar}{2}\right)\left(\frac{N_A}{m^*\varepsilon_s}\right)^{1/2}$.

Equation (3.27) describes the diode ideality factor as a result of tunneling enhanced recombination of electron hole pairs via an exponential distribution of recombination centers.

The dependence of the open circuit voltage V_{oc} on the recombination mechanism is [13-15]

$$V_{oc} \approx \frac{AkT}{q}\ln\left(\frac{J_{sc}}{J_{00}}\right) = \frac{E_a}{q} - \frac{AkT}{q}\ln\left(\frac{J_{00}}{J_{sc}}\right) . \tag{3.28}$$

If A and J_{00} in Eq. (3.28) are independent of temperature, the extrapolation to $T = 0$ K of the V_{oc} vs T plot gives the activation energy E_a which is the barrier height ϕ_b^p for interface recombination without tunneling. However, as soon as tunneling becomes important, resulting in temperature dependent of A, E_a is the band gap energy. A quantitative analysis of the temperature dependence of the diode ideality factor is required to decide in whether or not tunneling contributes significantly to recombination.

3.3 Conclusions

I have briefly described the general band diagram of heterojunction solar cells, the recombination current mechanism including the current transport model in ZnO/CdS/Cu(In,Ga)Se_2 heterojunction solar cell. From this model, it will be used to analyze the J-V curves resulting from the standard and temperature dependent J-V measurement in Chapter 5.

ศูนย์วิทยทรัพยากร
จุฬาลงกรณ์มหาวิทยาลัย